



OPEN ACCESS

EDITED BY

Ivan A. Paponov,
Aarhus University, Denmark

REVIEWED BY

Swen Schellmann,
University of Cologne, Germany
Jinbo Shen,
Zhejiang Agriculture and Forestry
University, China

*CORRESPONDENCE

Zhixiang Chen
✉ zhixiang@purdue.edu

[†]These authors have contributed equally to this work

SPECIALTY SECTION

This article was submitted to
Crop and Product Physiology,
a section of the journal
Frontiers in Plant Science

RECEIVED 23 November 2022

ACCEPTED 03 January 2023

PUBLISHED 17 January 2023

CITATION

Wang M, Luo S, Fan B, Zhu C and Chen Z
(2023) LIP5, a MVB biogenesis regulator, is
required for rice growth.
Front. Plant Sci. 14:1103028.
doi: 10.3389/fpls.2023.1103028

COPYRIGHT

© 2023 Wang, Luo, Fan, Zhu and Chen. This is an open-access article distributed under the terms of the [Creative Commons Attribution License \(CC BY\)](https://creativecommons.org/licenses/by/4.0/). The use, distribution or reproduction in other forums is permitted, provided the original author(s) and the copyright owner(s) are credited and that the original publication in this journal is cited, in accordance with accepted academic practice. No use, distribution or reproduction is permitted which does not comply with these terms.

LIP5, a MVB biogenesis regulator, is required for rice growth

Mengxue Wang^{1†}, Shuwei Luo^{1†}, Baofang Fan², Cheng Zhu¹
and Zhixiang Chen^{1,2*}

¹College of Life Science and Key Laboratory of Marine Food Quality and Hazard Controlling Technology of Zhejiang Province, China Jiliang University, Hangzhou, China, ²Department of Botany and Plant Pathology and Center for Plant Biology, Purdue University, West Lafayette, IN, United States

LYST-INTERACTING PROTEIN5 (LIP5) is a conserved regulator of multivesicular body (MVB) biogenesis in eukaryotes. In Arabidopsis, AtLIP5 is a target of stress-responsive MITOGEN-ACTIVATED PROTEIN KINASE3 and 6 and mediates stress-induced MVB biogenesis to promote stress responses. However, Arabidopsis *atlip5* knockout mutants are normal in growth and development. Here we report that rice *OsLIP5* gene could fully restore both the disease resistance and salt tolerance of the Arabidopsis *oslip5* mutant plants to the wild-type levels. Unlike Arabidopsis *atlip5* mutants, rice *oslip5* mutants were severely stunted, developed necrotic lesions and all died before flowering. Unlike in Arabidopsis, LIP5 regulated endocytosis under both stress and normal conditions in rice. These findings indicate that there is strong evolutionary divergence among different plants in the role of the conserved LIP5-regulated MVB pathway in normal plant growth.

KEYWORDS

multivesicular bodies, LYST-INTERACTING PROTEIN5, SKD1, rice, endocytosis, cellular homeostasis, plant growth

Introduction

Multivesicular bodies (MVBs) are late endosomes in the endocytic pathway (Cui et al., 2016). MVBs also mediate protein trafficking to the vacuole in the secretory pathway and are also called prevacuolar compartments in plants (Cui et al., 2016). MVBs are formed from trans-Golgi network/early endosomes by the invagination and budding of the limiting membrane into the lumen through the action of protein complexes named ESCRTs (endosomal sorting complexes required for transport) (Piper and Katzmann, 2007). MVB biogenesis is essential for plant growth and development and mutants for essential ESCRT components and associated factors such as SKD1 (SUPPRESSOR OF K⁺ TRANSPORT GROWTH DEFECT1) ATPase, which catalyzes the disassembly of the ESCRT III complex during MVB biogenesis, are lethal (Haas et al., 2007; Zhang et al., 2013; Gao et al., 2014). LYST-INTERACTING PROTEIN 5 (LIP5) is a conserved regulator of MVB biogenesis by activating the SKD1 ATPase (Haas et al., 2007; Skalicky et al., 2012; Guo and Xu, 2015; Vild et al., 2015). Importantly, Arabidopsis knockout mutants for *AtLIP5* have a largely normal phenotype in growth and development, indicating that the basal SKD1 activity is sufficient for MVB biogenesis under normal growth

conditions (Haas et al., 2007; Wang et al., 2014; Wang et al., 2015). However, the *atlip5* mutants are compromised both in stress-induced MVB formation and in disease resistance and stress tolerance (Wang et al., 2014; Wang et al., 2015; Xia et al., 2016). Arabidopsis AtLIP5 is subjected to degradation by the proteasome system under normal growth conditions but becomes stable under stress conditions upon phosphorylation by stress-responsive MITOGEN-ACTIVATED PROTEIN KINASE3 and 6 (MAPK3 and 6) to promote stress-induced MVB biogenesis (Wang et al., 2014; Wang et al., 2015). Thus, Arabidopsis AtLIP5 is a key regulator of stress-induced MVB biogenesis. Here, we have identified the functional homologue of the *LIP5* protein in rice through complementation of the Arabidopsis *atlip5* mutant plants. Furthermore, we have generated loss-of-function mutants for rice *OsLIP5* gene through CRISPR/Cas9. Surprisingly, the rice *oslip5* mutants were severely stunted, developed necrotic lesions and all died before flowering. Unlike in Arabidopsis, OsLIP5 regulated endocytosis under both stress and normal conditions in rice roots. The drastic difference in the *lip5* mutant phenotypes between Arabidopsis and rice raises an important question about the divergent functionality of LIP5-activated MVB pathway in plant growth and development under normal growth conditions.

Materials and methods

Plant materials and growth conditions

Arabidopsis (*Arabidopsis thaliana*) mutant and WT plants used in the study are all in the *Col-0* background. The *atlip5* mutants have been previously described (Lai et al., 2011; Wang et al., 2014). Arabidopsis were grown in growth chambers or rooms at 24°C, 120 $\mu\text{mol m}^{-2}\text{s}^{-1}$ light on a photoperiod of 12-hour light and 12-hour dark. Rice mutant and WT plants are in the background of rice cultivar Zhonghua 11. Rice plants were grown hydroponically in a modified rice culture solution containing 1.425 mM NH_4NO_3 , 0.2 mM NaH_2PO_4 , 0.513 mM K_2SO_4 , 0.998 mM CaCl_2 , 1.643 mM MgSO_4 , 0.009 mM MnCl_2 , 0.075 mM $(\text{NH}_4)_6\text{Mo}_7\text{O}_{24}$, 0.019 mM H_3BO_3 , 0.155 mM CuSO_4 , and 0.152 mM ZnSO_4 with 0.125 mM EDTA-Fe. pH 5.5 (Yoshida et al., 1976). Rice plants were grown in a growth room with a 14 h day (28°C)/10 h night (23°C) photoperiod at approximately 200 $\mu\text{mol m}^{-2}\text{s}^{-1}$ photon density, and approximately 60% humidity as described previously (Xu et al., 2017).

Identification rice *OsLIP5* gene and analysis of OsLIP5 subcellular localization

Rice *OsLIP5* gene was identified from the rice genome by BLASP search using Arabidopsis *OsLIP5* as a query with an e-value cutoff at $1\text{e}-10$. For subcellular localization of *OsLIP5*, full-length *OsLIP5* coding sequence was PCR-amplified from the rice cDNA using *OsLIP5*-specific primers (AGCCCATGGGGAGCGACGCGGAG and AGCTTAATTAATGAGTTTCGGCGGAAGG) and fused to the *GFP* gene behind the *CaMV* 35S promoter in a pFGC5941-derived binary plant expression vector (Li et al., 2021). Constructs for ARA6-mRFP and dexamethasone-inducible *SKD1* have been described previously (Wang et al., 2014). Colocalization analysis of AtLIP5 and

OsLIP5 with MVB marker ARA6 in *Nicotiana benthamiana* was performed as previously described (Wang et al., 2014).

Analysis of LIP5-SKD1 interactions using yeast two-hybrid assays

Full-length *OsLIP5* coding sequence was PCR amplified using gene-specific primers and cloned into yeast two-hybrid bait pAD-GAL4 vector as previously described (Wang et al., 2014). pBD-AtSKD1 bait and pAD-AtLIP5 prey constructs have been previously described (Wang et al., 2014). Various combinations of bait and prey constructs were co-transformed into yeast cells and interaction were analyzed by assaying *LacZ* β -galactosidase activity as described previously (Wang et al., 2014).

Complementation in Arabidopsis

For functional analysis through complementation of Arabidopsis *atlip5* mutant plants, the coding sequence of *OsLIP5* was PCR-amplified from rice cDNA using *OsLIP5*-specific primers and cloned into a pFGC5941-derived binary plant expression vector between the *CaMV* 35S promoter and a 4xmyc epitope tag (Li et al., 2021). The *OsLIP5* expression construct was introduced into the Arabidopsis *atlip5-1* mutant plants using the floral dipping method (Clough and Bent, 1998). Transgenic Arabidopsis plants were identified by their herbicide resistance to Basta. Expression of the transgene in the transgenic plants was analyzed by protein blotting using anti-myc monoclonal antibodies as previously described (Li et al., 2021).

Protein blotting

Protein isolation, electrophoretic separation, blotting and detection of LIP5-myc proteins using anti-myc antibodies were performed as previously described (Li et al., 2021).

Disease resistance and salt tolerance assays of Arabidopsis plants

Assays of Arabidopsis plant resistance to a virulent strain of *Pseudomonas syringae* pv *tomato* DC3000 (*Pst*DC3000) and tolerance to salt stress (150 mM NaCl) were performed as previously described (Wang et al., 2014; Wang et al., 2015).

Generation of Rice *OsLIP5* gene mutations using CRISPR/Cas9 genome editing

Two sites on the first and third exons of *OsLIP5*, both of which are close to the 5'-end of the *OsLIP5* coding sequence, were selected as targets for genome editing. The target sequences (ggcaTCGGCTCTACGCGATGGAGA/aaacTCTCCATCGCGTAGAGCCGA and ggcgGCAGACAAACAGGATCGTGC/aaagCACGAT

CCTGTTTGTCTGC) were inserted a rice CRISPR/Cas9 vector as previously described (Liu et al., 2020). Rice transformation into rice variety Zhonghua 11 was performed by co-cultivation of *hst1* rice calli with *Agrobacterium tumefaciens* strain EHA105 containing the CRISPR/cas9 construct as previously described (Hiei et al., 1994). For identification of mutations in the target sites, the regions were PCR-amplified using PCR primers flanking the regions from independent T1 transgenic lines and directly sequenced.

Analysis of endocytic activity in rice roots

Fluorescence microscopy of FM1-43 (Life Technologies) internalization in the roots of 7 days-old rice seedlings was also performed as described previously (Wang et al., 2014), with minor changes of the concentration of FM1-43 and staining time reduced to 10 μ M and 20 min, respectively. The wavelength settings of confocal microscopy were as follows: excitation at 488 nm and emission at 600 to 650 nm for FM1-43,

Results and discussion

OsLIP5 protein sequence, subcellular localization and interaction with SKD1

As in Arabidopsis, there is a single *LIP5* gene in the rice genome. The intron-exon architecture of rice *OsLIP5* is very similar to that of Arabidopsis *AtLIP5* (Figure 1A). The rice *OsLIP5* protein is also structurally highly homologous to Arabidopsis *AtLIP5* with 54% identity and 62% similarity in protein sequence (Figure 1B). *LIP5* binds a subset of ESCRT-III proteins through its N-terminal tandem microtubule-interacting and trafficking (MIT) domain and binds SKD1 ATPase through its C-terminal VSL (Vta1/SBP1/*LIP5*) domain (Haas et al., 2007; Spitzer et al., 2009; Skalicky et al., 2012; Wang et al., 2014). Sequence similarity is particularly high between *AtLIP5* and *OsLIP5* at these N- and C-terminal domains (Figure 1B). The middle segments of Arabidopsis and rice *LIP5* proteins are less conserved but both contain multiple Thr or Ser residues immediately preceding a Pro residues (TP or SP, Figure 1B), which are the phosphorylation sites of stress-responsive MAPK3/6 important for stress-induced *LIP5* protein stability in Arabidopsis (Wang et al., 2014; Wang et al., 2015).

To compare *OsLIP5* and *AtLIP5* for interaction with *AtSKD1*, we co-transformed yeast cells with a combination of pBD-*AtSKD1* bait construct with pAD-*AtLIP5*, pAD-*OsLIP5* or pAD empty prey vector. As shown in Figure 2C, yeast cells co-transformed with pBD-*AtSKD1* bait and pAD empty prey vectors had very low levels of *LacZ* reporter gene expression based on the β -galactosidase activity. On the other hand, yeast cells co-transformed with pBD-*AtSKD1* bait and pAD-*AtLIP5* or pAD-*OsLIP5* prey vectors contained similarly high β -galactosidase activity (Figure 1C). These results indicate that like *AtLIP5*, *OsLIP5* interacts strongly with *AtLIP5*.

To determine the subcellular localization of *OsLIP5*, we transiently expressed the *OsLIP5*-GFP construct in *N. benthamiana* and observed the GFP signals with confocal fluorescence microscopy. As previously observed with *AtLIP5*-GFP, the fluorescent signals from

the leaves expressing *OsLIP5*-GFP were largely cytosolic and diffusive. However, when co-expressed with *AtSKD1*, *OsLIP5*-GFP produced a large number of punctate fluorescent signals and approximately 60% of these signals were also labeled with co-expressed ARA6-mRFP MVB marker signals (Figure 1D). These results indicate that like *AtLIP5*, *OsLIP5* is associated with MVBs in the presence of SKD1.

Complementation of Arabidopsis *atlip5* mutant

To determine whether rice *OsLIP5* is a functional homolog of *AtLIP5*, we analyzed whether rice *OsLIP5* could rescue the defects of Arabidopsis *atlip5-1* mutant in disease resistance and salt tolerance. We generated the rice *OsLIP5* coding sequence fusion with a myc tag (*OsLIP5*-myc) and expressed it in Arabidopsis *atlip5-1* mutant under control of the *CaMV* 35S promoter. After infection with a virulent strain of the bacterial pathogen *Pseudomonas syringae*, the *atlip5* mutant plants developed stronger disease symptoms and supported higher bacterial growth than wild-type (WT) plants (Figures 2A, B). Expression of *OsLIP5*-myc completely restored the levels of resistance of the *atlip5* mutant to the WT levels (Figures 2A, B). When grown at 150 mM NaCl, both the cotyledon expansion and root growth of the *atlip5* mutant were greatly reduced when compared to those of WT (Figures 2C, D). Again, this compromised salt tolerance of *atlip5* was completely rescued by *OsLIP5*-myc (Figures 2C, D). At similar protein levels, *OsLIP5* was as effective as *AtLIP5* in restoring the disease resistance and salt tolerance of the *atlip5* mutant (Figure 2; Supplemental Figure 1). These results indicate that rice *OsLIP5* is a functional homolog of Arabidopsis *AtLIP5*.

Generation and characterization of rice *oslip5* mutants

To analyze the function of rice *OsLIP5* directly, we generated rice *oslip5* mutants by targeting two sites at the N-terminal domain of the *OsLIP5* protein using CRIPR/cas9-mediated genome editing. We obtained three heterozygous mutants (*oslip5-1*^{+/-}, *2*^{+/-} and *3*^{+/-}) that each contain a single base insertion at one of the two target sites (Figure 3A). The *oslip5-1* and *2* mutants contain an A and T insertions, respectively, between nucleotides 113 and 114 of the *OsLIP5* coding sequence (Figure 3B), which causes a reading frame shift and introduces a premature termination codon that is expected to produce a protein of 66 amino acid residues. The *oslip5-3* contains an A insertion between nucleotides 288-289 of the *OsLIP5* coding sequence, which causes a reading frame shift and introduces a premature termination codon that is expected to produce a protein of 115 amino acid residues (Figure 3B). The growth and development of all these three T1 heterozygous *oslip5*^{+/-} mutants were normal. In the T2 generation, three expected genotypes (WT, *oslip5*^{+/-} and *oslip5*^{-/-}) were segregated close to the expected 1:3:1 ratio for each mutant. The homozygous *oslip5*^{-/-} mutants germinated normally and grew similarly as WT during the first week post germination. However, starting from the second week post germination, the *oslip5*^{-/-} mutant seedlings became reduced in size relative to WT (Figure 4A). With

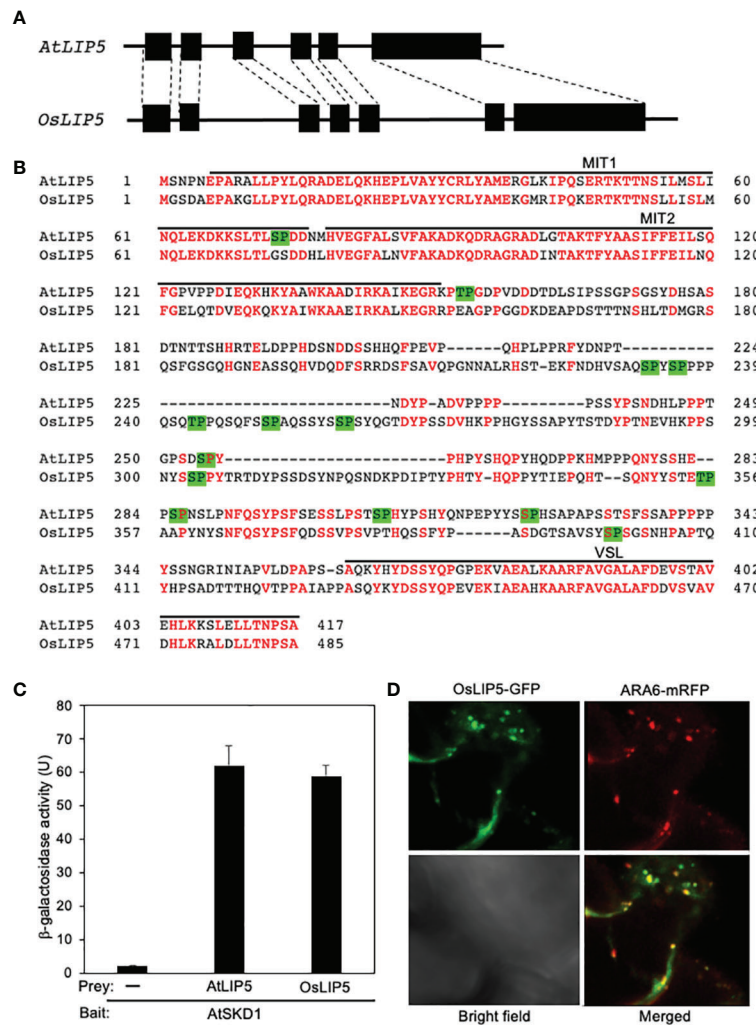


FIGURE 1

Gene structure, interaction with SKD1 and subcellular localization of rice LIP5. (A) Arabidopsis and rice LIP5 gene intron (line) and exon (box) architecture. The homologous exon between the Arabidopsis and rice LIP5 genes are indicated by dashed lines. (B) Amino acid sequence alignment of Arabidopsis and rice LIP5 proteins. Identical amino acid residues are in red. The N-terminal tandem MIT and C-terminal VSL domains are indicated. Putative TP and SP phosphorylation sites by proline-directed protein kinases are in green background. (C) Yeast two-hybrid assays of LIP5 proteins with AtSKD1. The indicated fusion bait and prey constructs were co-transformed into yeast cells. Empty pAD-Gal4 vector was used as negative control (-). Yeast transformants were analyzed for LacZ reporter gene expression through assays of β -galactosidase activity using ONPG (o-nitrophenyl- β -D-galactopyranose) as substrate. Data of arbitrary units (U) represent means and standard errors ($n=5$). (D) Subcellular colocalization of OsLIP5-GFP with ARA6-mRFP when co-expressed with AtSKD1 in the leaf epidermal cells of *N. benthamiana*.

increased age, the stunted growth of the *oslip5*^{-/-} mutants became more pronounced based on the increased difference of their sizes from those of WT (Figure 4A; Supplemental Figure 2). After 3 weeks post germination the leaves of the *oslip5*^{-/-} mutant seedlings also developed necrotic lesions, which spread rapidly during the following 2-3 weeks (Figure 4A; Supplemental Figure 2). All the *oslip5*^{-/-} mutant seedlings died in 6-8 weeks post germinations (Figure 4A) and, therefore, the mutations could only be maintained in the *oslip5*^{+/-} heterozygous state. These *oslip5*^{-/-} mutant seedlings were grown hydroponically or in soil in greenhouses or growth chambers under highly favorable conditions but they were always stunted in growth, developed lesions and all died before flowering. The strong growth defects and premature death of the *oslip5*^{-/-} mutants were observed in the subsequent generations. Thus, unlike Arabidopsis AtLIP5, rice OsLIP5 is required for rice growth and survival even under normal growth conditions.

Role of rice OsLIP5 in basal and stress-induced endocytosis

As late endosomes in the endocytic pathway, MVB biogenesis directly affects endocytosis (Stahl and Barbieri, 2002). Using the styryl dye FM1-43 as a fluorescent endocytosis marker, we have previously demonstrated that the basal endocytosis under normal growth conditions was largely normal in the Arabidopsis *atlip5* mutants (Wang et al., 2014; Wang et al., 2015). However, in salt-treated roots, the endocytic activity was induced by about 3-fold in Arabidopsis WT but only about 30% in the *atlip5* mutants (Wang et al., 2015). Likewise, pathogen-induced endocytosis was greatly compromised in the Arabidopsis *atlip5* mutants (Wang et al., 2014). These results indicate that Arabidopsis AtLIP5 is a key regulator for pathogen- and stress-induced MVB biogenesis upon exposure to pathogens and abiotic stress. The role of Arabidopsis AtLIP5 as a specific activator of stress-

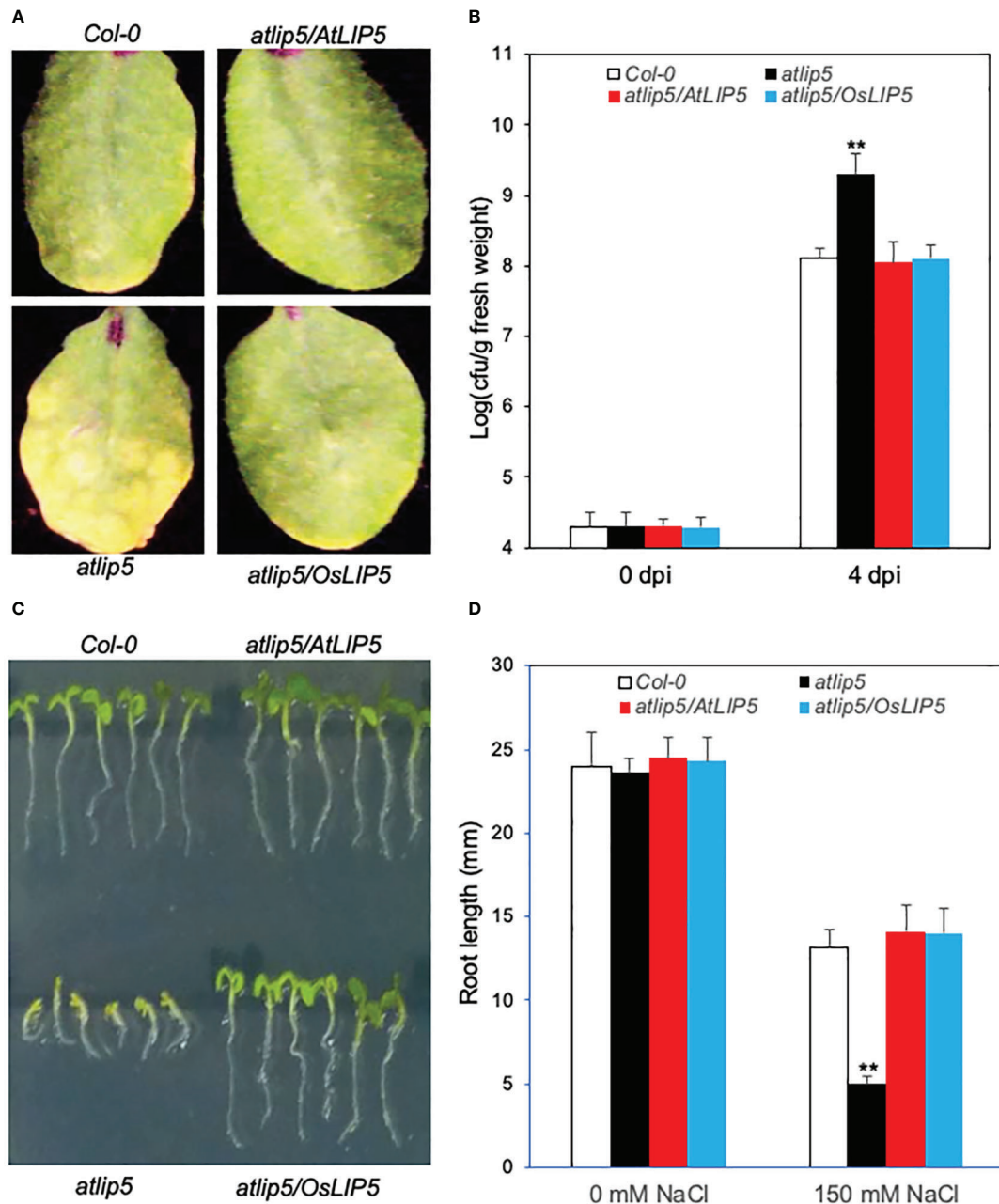


FIGURE 2

Complementation of Arabidopsis *atlip5-1* mutant by rice *OsLIP5*. Disease symptom development after infection by the virulent *P. syringae* pv *tomato* DC3000 (*Pst*DC3000). Arabidopsis Col-0 WT, *atlip5-1* and *atlip5-1/AtLIP5* and *atlip5-1/OsLIP5* lines with similar levels of LIP5-myc proteins were inoculated with *Pst*DC3000 ($OD_{600} = 0.0002$ in 10 mM $MgCl_2$). Pictures of representative leaves were taken at 4 days post inoculation (dpi) (A). Leaf samples were taken at 0 or 4 dpi to determine the bacterial growth (B). The means and standard errors were calculated from 10 plants for each mutant. Double asterisks indicate statistically significant difference at $P < 0.01$ in the colony forming units (cfu) per gram leaf fresh weight between Col-0 WT and *atlip5* mutant lines determined at the same dpi. Arabidopsis seeds for the above genotypes were surface sterilized and sown on one-half-strength MS medium supplemented with 150mM NaCl. Photographs were taken 2 days post stratification and 5 days post germination (C). Root length of seedlings determined at 5 days post germination (D). Means and standard errors were calculated from three experiments. Double asterisks indicate statistically significant difference at $P < 0.01$ in root length between Col-0 WT and *atlip5* mutant lines with the same salt treatment.

induced MV biogenesis and endocytosis is consistent with the normal growth and development but compromised disease resistance and stress tolerance of the *atlip5* mutants (Wang et al., 2014; Wang et al., 2015). Because of the drastic difference in the growth phenotypes of the *lip5* mutants between Arabidopsis and rice, we also compared rice WT and *oslip5* mutants for both basal and stress-induced endocytosis using FM1-43 as a marker. The membrane-selective FM1-43, which fluoresces only in a lipid-rich membrane, can enter the cells by

endocytic vesicles derived from the plasma membrane (Schikorski, 2010; Amaral et al., 2011). Initial attempts to analyze the endocytic activity using FM1-43 in rice sheaths generated unreproducible results likely due to wounding and other stresses generated during FM1-43 infiltration and preparation of sheath slices. We subsequently compared WT and *oslip5* mutant roots for internalized FM1-43 signal after 20 minutes of incubation with or without prior salt treatment. Importantly, we observed significantly higher levels of

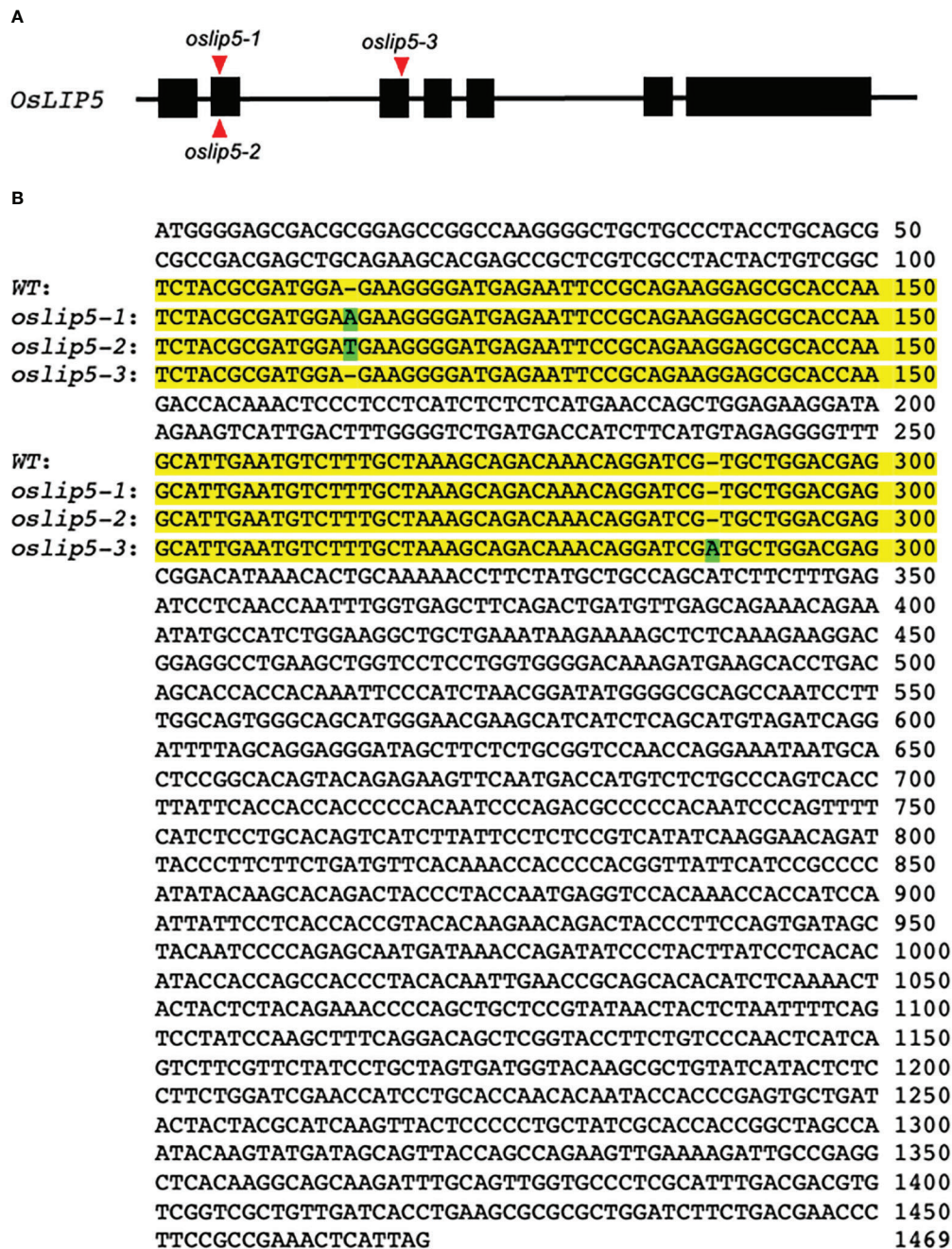


FIGURE 3

Targeted mutations of rice *OsLIP5* gene using CRISPR/cas9 genome editing. (A) Rice *OsLIP5* gene structure and the positions of three *oslip5* mutations on their genomic sequences as indicated by red arrowheads. (B) Comparison of *OsLIP5* coding sequences in WT and three *oslip5* mutants. The two target sides containing the mutations are in yellow background. Inserted basis in the three *oslip5* mutants are in green background.

internalized FM1-43 signal in WT roots than in the *oslip5* mutant roots even without salt treatment (Figures 4B, C). With salt treatment (at 150 mM NaCl), the intensity of internalized FM1-43 fluorescence signal increased by almost 4-fold in WT roots but only by about 35% in the *oslip5* mutant roots (Figures 4B, C). Thus, unlike in Arabidopsis, where mutations of *AtLIP5* affected only stress-induced endocytosis (Wang et al., 2014; Wang et al., 2015), the mutations of *OsLIP5* impacted both basal and stress-induced endocytosis in rice. Thus, the differential growth phenotypes of the *lip5* mutants are correlated with the differential roles of LIP5 proteins in the basal endocytosis under the normal growth conditions between Arabidopsis and rice.

What could be the molecular and evolutionary basis for the differential roles of LIP5 in plant growth and endocytosis in different plants? In Arabidopsis *atlip5* mutant roots, despite normal basal endocytosis when assayed using FM1-43 as marker, there are defects in the trafficking of auxin efflux transporters (Buono et al., 2016), indicating that even Arabidopsis *AtLIP5* has a role in the trafficking and turnover of specific plasma membrane proteins under normal growth conditions. Besides LIP5, there are other regulators of SKD1 and MVB biogenesis such as IST1-like proteins in Arabidopsis and the lack of strong growth phenotype of Arabidopsis *atlip5* mutants could be due to functional redundancy among these MVB

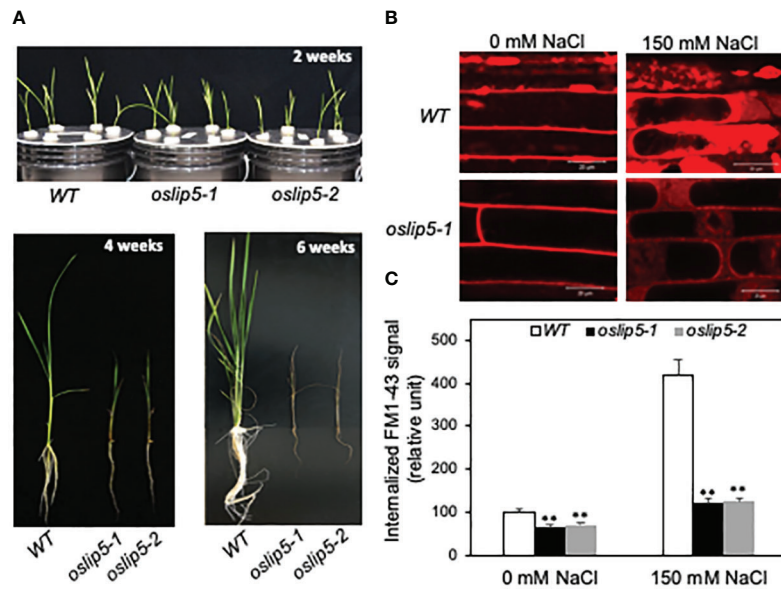


FIGURE 4

Phenotypes of rice WT, *oslip5* mutants in growth and endocytosis. Comparison of growth of 2-, 4- and 6-week-old rice WT, *oslip5-1* and *oslip5-2* mutants grown hydroponically under normal growth conditions (A). Five-day-old rice seedlings were treated with 0 or 150 mM NaCl for 20 h. Basal and salt-induced endocytosis was analyzed using FM1-43 as indicated by the representative confocal images of rice root epidermal cells after FM1-43 staining (B). Bars =20 μ m. The fluorescent signal intensity of internalized FM1-43 was determined from 20 Z stack images of root epidermal cells (C). Means and SE were calculated from images of 10 independent roots (20 images per root). Double asterisks indicate statistically significant difference at $P < 0.01$ in the levels of internalized FM1-43 signal between Col-0 WT and *atlip5* mutant lines with the same salt treatment.

regulators. Consistent with this possibility, while Arabidopsis *atlip5* and *atist1-like1(atistl1)* single mutants are largely normal in growth and development, the *atlip5/atistl1* double mutant is severely stunted in growth, develops spontaneous cell death and cannot produce seeds (Buono et al., 2016). Arabidopsis LIP5 also functionally interacts with FYVE4, a plant-unique ESCRT component and regulator of MVB biogenesis (Liu et al., 2021). An Arabidopsis *fyve4* null mutant displays modestly reduced growth and early senescence but its double mutant with *atlip5* is seedling lethal (Liu et al., 2021). It remains to be determined whether the patterns of functional interactions among different regulators of MVB biogenesis might vary in different plants. If OSLIP5 acts as a major regulator of MVB biogenesis under normal growth conditions with relatively low functional redundancy with other MVB regulators in rice, its loss-of-function would have an important effect on rice growth and reproduction as observed in the *oslip5* mutants.

The drastically different phenotypes between the Arabidopsis and rice *lip5* mutants could also be attributed to the diversity among different plant species in their adaptability to perturbed cellular homeostasis. It is known that MVB pathway and related autophagy participate in plant stress responses by targeting vacuolar degradation of damaged, harmful and unwanted proteins and cellular constituents, which are often elevated under biotic and abiotic stress conditions (Li et al., 2018; Luo et al., 2021). Under normal growth conditions, however, cells also generate damaged, harmful and unwanted cellular constituents, which require prompt turnover for robust plant growth and development. In the endoplasmic reticulum (ER), about 30% of all proteins produced are misfolded under homeostatic conditions (Fink, 1999), which are mostly degraded by ER-associated degradation in the proteasome. In chloroplasts, the process of photosynthesis leads to production of

damaged proteins under normal growth conditions, which are removed by both intraplasmic proteases and extraplasmic pathways including autophagy (Izumi and Nakamura, 2018). In different plant species, there could be divergence in the complex cellular networks that function in maintaining cellular homeostasis to promote growth and development. In addition, while Arabidopsis is a wild plant, rice is a crop plant that has been intensively selected artificially to increase yield and other human needs and may have evolved heightened levels of the vacuolar degradation pathways to promote growth and reproduction.

Autophagy is also a conserved degradation pathway closely related to MVB-dependent endocytosis by delivering cytoplasmic components to the lysosome/vacuole for degradation (Cui et al., 2018). In Arabidopsis, like LIP5-activated MVB pathway, autophagy is stress-inducible and autophagy mutants are strongly compromised in disease resistance and stress tolerance. Despite extensive alterations in transcriptomes, proteasomes and metabolomes, Arabidopsis autophagy-deficient mutants are largely normal in growth and reproduction (Masclaux-Daubresse et al., 2014; Mcloughlin et al., 2018; Have et al., 2019; Mcloughlin et al., 2020). In rice, however, autophagy mutants are male sterile due to defects in degradation of the tapetum and pollen maturation (Kurusu et al., 2014). Interestingly, while Arabidopsis AtLIP5-mediated MVB pathway plays a critical positive role in disease resistance, rice LRD6-6 regulates MVB-mediated trafficking to inhibit biosynthesis of antimicrobial compounds and immunity in rice (Zhu et al., 2016). Therefore, the two most extensively analyzed model plants appear to differ greatly in the way by which these two conserved vacuolar degradation pathways participate in plant growth, development and stress responses. Further analysis of the strong plant diversity in coping with perturbed cellular homeostasis could provide important

new insights into the genetic and molecular basis important for both plant survival under stress condition and plant growth and productivity under normal growth conditions.

Data availability statement

The original contributions presented in the study are included in the article/[Supplementary Material](#). Further inquiries can be directed to the corresponding author.

Author contributions

ZC and CZ conceived the project and designed the research. MW and SL performed most of the experiments. BF performed some of the experiments. MW, SL and ZC wrote the manuscript. All authors contributed to the article and approved the submitted version.

Funding

This work is supported by China National Major Research and Development Plan (grant no. 0111900), National Natural Science Foundation of China (grant no. 32000143) and Zhejiang Provincial

Natural Science Foundation of China (grant no. LQ20C020002) at China Jiliang University.

Conflict of interest

The authors declare that the research was conducted in the absence of any commercial or financial relationships that could be construed as a potential conflict of interest.

Publisher's note

All claims expressed in this article are solely those of the authors and do not necessarily represent those of their affiliated organizations, or those of the publisher, the editors and the reviewers. Any product that may be evaluated in this article, or claim that may be made by its manufacturer, is not guaranteed or endorsed by the publisher.

Supplementary material

The Supplementary Material for this article can be found online at: <https://www.frontiersin.org/articles/10.3389/fpls.2023.1103028/full#supplementary-material>

References

- Amaral, E., Guatimosim, S., and Guatimosim, C. (2011). Using the fluorescent styryl dye FM1-43 to visualize synaptic vesicles exocytosis and endocytosis in motor nerve terminals. *Methods Mol. Biol.* 689, 137–148. doi: 10.1007/978-1-60761-950-5_8
- Buono, R. A., Paez-Valencia, J., Miller, N. D., Goodman, K., Spitzer, C., Spalding, E. P., et al. (2016). Role of SKD1 regulators LIP5 and IST1-LIKE1 in endosomal sorting and plant development. *Plant Physiol.* 171, 251–264. doi: 10.1104/pp.16.00240
- Clough, S. J., and Bent, A. F. (1998). Floral dip: a simplified method for agrobacterium-mediated transformation of arabidopsis thaliana. *Plant J.* 16, 735–743. doi: 10.1046/j.1365-3113x.1998.00343.x
- Cui, Y., He, Y., Cao, W., Gao, J., and Jiang, L. (2018). The multivesicular body and autophagosome pathways in plants. *Front. Plant Sci.* 9. doi: 10.3389/fpls.2018.01837
- Cui, Y., Shen, J., Gao, C., Zhuang, X., Wang, J., and Jiang, L. (2016). Biogenesis of plant prevacuolar multivesicular bodies. *Mol. Plant* 9, 774–786. doi: 10.1016/j.molp.2016.01.011
- Fink, A. L. (1999). Chaperone-mediated protein folding. *Physiol. Rev.* 79, 425–449. doi: 10.1152/physrev.1999.79.2.425
- Gao, C., Luo, M., Zhao, Q., Yang, R., Cui, Y., Zeng, Y., et al. (2014). A unique plant ESCRT component, FREE1, regulates multivesicular body protein sorting and plant growth. *Curr. Biol.* 24, 2556–2563. doi: 10.1016/j.cub.2014.09.014
- Guo, E. Z., and Xu, Z. (2015). Distinct mechanisms of recognizing endosomal sorting complex required for transport III (ESCRT-III) protein IST1 by different microtubule interacting and trafficking (MIT) domains. *J. Biol. Chem.* 290, 8396–8408. doi: 10.1074/jbc.M114.607903
- Haas, T. J., Sliwinski, M. K., Martinez, D. E., Preuss, M., Ebine, K., Ueda, T., et al. (2007). The arabidopsis AAA ATPase SKD1 is involved in multivesicular endosome function and interacts with its positive regulator LYST-INTERACTING PROTEIN5. *Plant Cell* 19, 1295–1312. doi: 10.1105/tpc.106.049346
- Have, M., Luo, J., Tellier, F., Balliau, T., Cueff, G., Chardon, F., et al. (2019). Proteomic and lipidomic analyses of the arabidopsis atg5 autophagy mutant reveal major changes in endoplasmic reticulum and peroxisome metabolisms and in lipid composition. *New Phytol.* 223, 1461–1477. doi: 10.1111/nph.15913
- Hiei, Y., Ohta, S., Komari, T., and Kumashiro, T. (1994). Efficient transformation of rice (*Oryza sativa* L.) mediated by agrobacterium and sequence analysis of the boundaries of the T-DNA. *Plant J.* 6, 271–282. doi: 10.1046/j.1365-3113x.1994.6020271.x
- Izumi, M., and Nakamura, S. (2018). Chloroplast protein turnover: The influence of extraplasmidic processes, including autophagy. *Int. J. Mol. Sci.* 19, 828. doi: 10.3390/ijms19030828
- Kurusu, T., Koyano, T., Hanamata, S., Kubo, T., Noguchi, Y., Yagi, C., et al. (2014). OsATG7 is required for autophagy-dependent lipid metabolism in rice postmeiotic anther development. *Autophagy* 10, 878–888. doi: 10.4161/auto.28279
- Lai, Z., Wang, F., Zheng, Z., Fan, B., and Chen, Z. (2011). A critical role of autophagy in plant resistance to necrotrophic fungal pathogens. *Plant J. Cell Mol. Biol.* 66, 953–968. doi: 10.1111/j.1365-3113x.2011.04553.x
- Li, X., Bao, H., Wang, Z., Wang, M., Fan, B., Zhu, C., et al. (2018). Biogenesis and function of multivesicular bodies in plant immunity. *Front. Plant Sci.* 9, 979. doi: 10.3389/fpls.2018.00979
- Liu, C., Zeng, Y., Li, H., Yang, C., Shen, W., Xu, M., et al. (2021). A plant-unique ESCRT component, FYVE4, regulates multivesicular endosome biogenesis and plant growth. *New Phytol.* 231, 193–209. doi: 10.1111/nph.17358
- Liu, X., Zhou, X., Li, K., Wang, D., Ding, Y., Liu, X., et al. (2020). A simple and efficient cloning system for CRISPR/Cas9-mediated genome editing in rice. *PeerJ* 8, e8491. doi: 10.7717/peerj.8491
- Li, X., Wang, Z., Fu, Y., Cheng, X., Zhang, Y., Fan, B., et al. (2021). Two ubiquitin-associated ER proteins interact with COPT copper transporters and modulate their accumulation. *Plant Physiol.* 187, 2469–2484. doi: 10.1093/plphys/kiab381
- Luo, S. W., Li, X. F., Zhang, Y., Fu, Y. T., Fan, B. F., Zhu, C., et al. (2021). Cargo recognition and function of selective autophagy receptors in plants. *Int. J. Mol. Sci.* 22, 1013. doi: 10.3390/ijms22031013
- Masclaux-Daubresse, C., Clement, G., Anne, P., Routaboul, J. M., Guiboileau, A., Soulay, F., et al. (2014). Stitching together the multiple dimensions of autophagy using metabolomics and transcriptomics reveals impacts on metabolism, development, and plant responses to the environment in arabidopsis. *Plant Cell* 26, 1857–1877. doi: 10.1105/tpc.114.124677
- Mcloughlin, F., Augustine, R. C., Marshall, R. S., Li, F., Kirkpatrick, L. D., Otegui, M. S., et al. (2018). Maize multi-omics reveal roles for autophagic recycling in proteome remodelling and lipid turnover. *Nat. Plants* 4, 1056–1070. doi: 10.1038/s41477-018-0299-2
- Mcloughlin, F., Marshall, R. S., Ding, X., Chatt, E. C., Kirkpatrick, L. D., Augustine, R. C., et al. (2020). Autophagy plays prominent roles in amino acid, nucleotide, and carbohydrate metabolism during fixed-carbon starvation in maize. *Plant Cell* 32, 2699–2724. doi: 10.1105/tpc.20.00226
- Piper, R. C., and Katzmman, D. J. (2007). Biogenesis and function of multivesicular bodies. *Annu. Rev. Cell Dev. Biol.* 23, 519–547. doi: 10.1146/annurev.cellbio.23.090506.123319

- Schikorski, T. (2010). Monitoring rapid endocytosis in the electron microscope via photoconversion of vesicles fluorescently labeled with FM1-43. *Methods Mol. Biol.* 657, 329–346. doi: 10.1007/978-1-60761-783-9_26
- Skalicky, J. J., Arai, J., Wenzel, D. M., Stubblefield, W. M., Katsuyama, A., Uter, N. T., et al. (2012). Interactions of the human LIP5 regulatory protein with endosomal sorting complexes required for transport. *J. Biol. Chem.* 287, 43910–43926. doi: 10.1074/jbc.M112.417899
- Spitzer, C., Reyes, F. C., Buono, R., Sliwinski, M. K., Haas, T. J., and Otegui, M. S. (2009). The ESCRT-related CHMP1A and b proteins mediate multivesicular body sorting of auxin carriers in arabidopsis and are required for plant development. *Plant Cell* 21, 749–766. doi: 10.1105/tpc.108.064865
- Stahl, P. D., and Barbieri, M. A. (2002). Multivesicular bodies and multivesicular endosomes: the “ins and outs” of endosomal traffic. *Sci. STKE* 2002, pe32. doi: 10.1126/stke.2002.141.pe3
- Vild, C. J., Li, Y., Guo, E. Z., Liu, Y., and Xu, Z. (2015). A novel mechanism of regulating the ATPase VPS4 by its cofactor LIP5 and the endosomal sorting complex required for transport (ESCRT)-III protein CHMP5. *J. Biol. Chem.* 290, 7291–7303. doi: 10.1074/jbc.M114.616730
- Wang, F., Shang, Y., Fan, B., Yu, J. Q., and Chen, Z. (2014). Arabidopsis LIP5, a positive regulator of multivesicular body biogenesis, is a critical target of pathogen-responsive MAPK cascade in plant basal defense. *PLoS Pathog.* 10, e1004243. doi: 10.1371/journal.ppat.1004243
- Wang, F., Yang, Y., Wang, Z., Zhou, J., Fan, B., and Chen, Z. (2015). A critical role of lyst-interacting Protein5, a positive regulator of multivesicular body biogenesis, in plant responses to heat and salt stresses. *Plant Physiol.* 169, 497–511. doi: 10.1104/pp.15.00518
- Xia, Z., Huo, Y., Wei, Y., Chen, Q., Xu, Z., and Zhang, W. (2016). The arabidopsis LYST INTERACTING PROTEIN 5 acts in regulating abscisic acid signaling and drought response. *Front. Plant Sci.* 7, 758. doi: 10.3389/fpls.2016.00758
- Xu, L., Zhao, H., Ruan, W., Deng, M., Wang, F., Peng, J., et al. (2017). ABNORMAL INFLORESCENCE MERISTEM1 functions in salicylic acid biosynthesis to maintain proper reactive oxygen species levels for root meristem activity in rice. *Plant Cell* 29, 560–574. doi: 10.1105/tpc.16.00665
- Yoshida, S., Forno, D. A., Cook, J. H., and Gomez, K. A. (1976). “Routine procedures for growing rice plants in culture solution,” in *Laboratory manual for physiological studies of rice*. Eds. S. Yoshida, D. A. Forno, J. H. Cook and K. A. Gomez (Los Banos, Philippines: International Rice Research Institute), 61–66.
- Zhang, X. Q., Hou, P., Zhu, H. T., Li, G. D., Liu, X. G., and Xie, X. M. (2013). Knockout of the VPS22 component of the ESCRT-II complex in rice (*Oryza sativa* L.) causes chalky endosperm and early seedling lethality. *Mol. Biol. Rep.* 40, 3475–3481. doi: 10.1007/s11033-012-2422-1
- Zhu, X., Yin, J., Liang, S., Liang, R., Zhou, X., Chen, Z., et al. (2016). The multivesicular bodies (MVBs)-localized AAA ATPase LRD6-6 inhibits immunity and cell death likely through regulating MVBs-mediated vesicular trafficking in rice. *PLoS Genet.* 12, e1006311. doi: 10.1371/journal.pgen.1006311